

Supplementary Information for

**RNA sequencing reveals novel macrophage transcriptome favoring neurovascular plasticity after ischemic stroke**

Rongrong Wang, Yaan Liu, Qing Ye, Sulaiman H. Hassan, Jingyan Zhao, Sicheng Li, Xiaoming Hu, Rehana K. Leak, Marcelo Rocha, Lawrence R. Wechsler, Jun Chen, and Yejie Shi

Corresponding author: Yejie Shi

Email: [y.shi@pitt.edu](mailto:y.shi@pitt.edu)

**This PDF file includes:**

Supplementary Methods

Supplementary Figure 1

Supplementary Tables 1-8

Supplementary References

## Supplementary Methods

### *Choose of sample size*

Sample sizes for the bulk RNA sequencing experiments were determined based what is commonly used for this technique in the literature. The number of animals required for the *in vivo* studies was determined by power analysis based on our experience with the murine dMCAO model. To detect a 30% decrease in infarct volume or neurological deficits with 80% power at an  $\alpha$  value of 0.05 (two-tailed), approximately 6-8 mice per group was needed. For flow cytometry and immunohistochemistry, 4 samples were required for 80% power ( $\beta=0.8$ ,  $\alpha=0.05$ ) to detect a 30% change after dMCAO.

### *Permanent focal cerebral ischemia*

Focal cerebral ischemia was induced in mice (8-12 weeks old, 25-30 g) by permanent occlusion of the left distal middle cerebral artery (MCA) and left common carotid artery (CCA), as described previously.<sup>1,2</sup> We refer to this model as distal MCA occlusion (dMCAO). Briefly, a skin incision was made at the midline of the neck, and the left CCA was exposed and ligated. A craniotomy was performed between the left eye and the ear, to expose the conjunction of the rhinal fissure and MCA. The distal branch of the left MCA was then occluded with low intensity bipolar electrocautery at the immediate lateral part of the rhinal fissure. Both the rectal temperature and the left temporalis muscle temperature were maintained at  $37.0\pm 0.5^{\circ}\text{C}$  during surgery with a temperature-controlled heating pad and a heat lamp. Mean arterial blood pressure was monitored during surgery by a tail cuff. Cortical cerebral blood flow (CBF) was monitored using two-dimensional laser speckle techniques, according to the manufacturer's instructions, as before.<sup>3</sup> Failure to reduce CBF to 30% or less of baseline levels or death immediately after ischemia led to subject exclusion (<10%), and these exclusions were spread out evenly in all stroke groups. Sham-operated animals underwent the same anesthesia and surgical procedures, with the exception of occlusion of the CCA and MCA.

Experimental procedures were performed following criteria derived from *Stroke Therapy Academic Industry Roundtable* (STAIR) group guidelines for preclinical evaluation of stroke therapeutics. Accordingly, experimental group assignments were randomized with a lottery-

drawing box, and surgeries and all outcome assessments were performed by investigators blinded to genotype and group assignments.

### ***Fluorescence-activated cell sorting (FACS)***

Single-cell suspensions were prepared from mouse blood and brain, as described previously.<sup>4</sup> Briefly, peripheral blood was obtained from deeply anesthetized mice by cardiac puncture, and 700  $\mu$ L of blood was diluted in 1300  $\mu$ L of HBSS and 100  $\mu$ L of 1% heparin sodium. The diluted blood was fractionated in 2 mL Ficoll solution at 500 g for 15 min. Mononuclear cells in the middle layer were collected. Mice were transcardially perfused with sterile 0.9% NaCl after blood collection. The ipsilesional brain hemisphere was harvested, and cell suspensions were prepared using the Neural Tissue Dissociation Kit and gentleMACS Octo Dissociator with Heaters (Miltenyi Biotec) according to the manufacturer's instructions. Suspensions were passed through a 70  $\mu$ m cell strainer, and fractionated on a 30% and 70% Percoll gradient at 500 g for 30 min. Mononuclear cells at the interface were collected. Isolated mononuclear cells were washed, resuspended at  $1 \times 10^6$  per mL, and stained with fluorophore-conjugated antibodies and the appropriate isotype controls (Supplementary Table 1). Flow cytometry was performed using the FACS Aria I sorter and FACS Diva software (BD Biosciences). Monocytes and macrophages were gated as CD11c<sup>-</sup>Ly6G<sup>-</sup>CD11b<sup>+</sup>CD45<sup>high</sup> and sorted for bulk RNA-seq. For blood monocytes, each sample was extracted from one mouse. For brain macrophages, each sample was pooled from 5 mouse brains. Flow cytometry data were analyzed using FlowJo software.

### ***RNA sequencing***

RNA extraction, library preparation, and sequencing were performed at the University of Pittsburgh HSCRF Genomics Research Core. Briefly, total RNA was extracted from FACS-sorted cells using RNeasy Plus Micro Kit (Qiagen), according to the manufacturer's instructions. RNA integrity was assessed using the High Sensitivity RNA ScreenTape system on an Agilent 2200 TapeStation. The SMART-Seq HT Kit was used to generate cDNA from 10 ng of total RNA, and the cDNA product was checked by an Agilent Fragment Analyzer system for quality control. The sequencing library was constructed by following the Illumina Nextera XT Sample Preparation Guide. One nanogram of input cDNA was tagmented (tagged and fragmented) and amplified using the Illumina Nextera XT kit. Sequence libraries of each sample were finally

equimolarly pooled and sequenced on an Illumina Nextseq 500 system, using a paired-end 75-bp strategy.

### ***RNA-seq data analysis***

#### *Preprocessing.*

Preprocessing of the bulk RNA-seq data was completed using *Chipster*.<sup>5</sup> Fastq files were quality controlled using *FastQC*.<sup>6</sup> All samples passed quality control criteria. Reads were mapped to the GRCm38 mouse genome using *HISAT2*<sup>7</sup> and counted by *HTSeq*.<sup>8</sup> Genes were identified by Ensembl ID.<sup>9</sup> Read counts were subsequently analyzed using R/Bioconductor.<sup>10</sup>

#### *Differential expression analysis.*

The R package *DESeq2*<sup>11</sup> was used to normalize the counts and to perform differential expression analysis. Differentially expressed genes (DEGs) were defined as genes with a fold change  $>2$  or  $<-2$ , and with a Benjamini-Hochberg adjusted p-value  $<0.05$ . Normalized read counts were used for gene expression profiling and were  $\log_2(x+1)$ -transformed. For principal component analysis (PCA), variance-stabilizing transformation was performed on normalized counts for each sample. Heatmaps were generated using the R package *pheatmap*. Normalized counts were log transformed, z-scaled, and used as input data for heatmap construction. Hierarchical clustering was performed using the ward.D2 method, based on the Euclidean distances between cluster means.

#### *Functional enrichment analysis.*

Functional enrichment analysis was performed using the online tool *Metascape*<sup>12</sup> and the R package *clusterProfiler*.<sup>13</sup> All genes in the mouse genome were used as the enrichment background. *Metascape* returns a list of significantly overrepresented ( $p < 0.01$ ) ontology terms with a minimum count of 3, and an enrichment factor (the ratio between the observed counts and the counts expected by chance) larger than 1.5. Terms were grouped into clusters based on their membership similarities, and rendered as a network plot, where terms with a similarity  $> 0.3$  were connected by edges. Additional gene ontology (GO) enrichment analysis was performed using the R package *clusterProfiler*. A term was considered significantly enriched with a Benjamini-Hochberg adjusted p-value  $<0.01$ . Enriched terms were visualized as dot plots, where

the color and size of a dot represented its adjusted p-value and gene count, respectively. Alternatively, enrichment data were visualized as bubble plots, circular plots, or Circos plots using the R package *GOpilot*.<sup>14</sup>

#### *Ingenuity Pathway Analysis (IPA).*

DEGs identified by *DESeq2* were submitted to IPA for pathway analysis using the Ingenuity Knowledge Base (Qiagen Bioinformatics).<sup>15</sup> The fold change and adjusted p-value for each gene were used to perform the core analysis. The Upstream Regulator analysis was used to identify the cascade of upstream transcriptional regulators that can explain the observed gene expression changes in the dataset. An upstream regulator was predicted to be strongly activated or inhibited if its activation z-score was larger than 2 or smaller than -2, respectively. The cutoff of p-value was set at 0.01.

#### ***Immunohistochemistry and data analyses***

Mice were deeply anesthetized and transcardially perfused with 0.9% NaCl, followed by 4% paraformaldehyde in PBS. Brains were harvested and cryoprotected in 30% sucrose in PBS, and frozen serial coronal brain sections (25- $\mu$ m thick) were prepared on a sliding microtome (Microm HM 450, Thermo Scientific). Sections were blocked with 5% donkey serum in PBS for 1 h, followed by overnight incubation (4°C) with primary antibodies (Supplementary Table 1). After washing, sections were incubated for 1 h at 20°C with donkey secondary antibodies conjugated with DyLight 488 or Cy3 fluorophores (1:1000, Jackson ImmunoResearch Laboratories). Alternate sections from each experimental condition were incubated in all solutions except the primary antibodies to assess nonspecific secondary antibody staining. Nuclei were then counterstained with DAPI for 2 min at 20°C, mounted, and coverslipped with Fluoromount-G (Southern Biotech). Fluorescence images were captured with an inverted Nikon Diaphot-300 fluorescence microscope equipped with a SPOT RT slider camera and Meta Series Software 5.0 (Molecular Devices), or with an Olympus Fluoview FV1000 confocal microscope and FV10-ASW 2.0 software.

Neuronal tissue loss was measured using ImageJ on six equally spaced sections encompassing the MCA territory immunostained for microtubule-associated protein 2 (MAP2).

Cortical tissue loss was calculated as the volume of the MAP2-immunopositive contralesional cerebral cortex minus that of the ipsilesional cortex.

### ***Examination of newly proliferated cells***

Newly proliferated cells were labeled with the S-phase marker 5-bromo-2'-deoxyuridine (BrdU) as previously described.<sup>16</sup> Briefly, mice received intraperitoneal injections of BrdU twice a day at a dose of 50 mg/kg body weight at 3-6 days after dMCAO. At 35 days after dMCAO, brains were cut into coronal sections and immunostained with an anti-BrdU antibody, as before.<sup>16</sup> BrdU-immunopositive cells were counted using ImageJ and calculated as the number of cells in the designated fields divided by the area (mm<sup>2</sup>) of the fields. Neurogenesis was evaluated on BrdU/NeuN double-stained sections. Angiogenesis was assessed by counting BrdU immunopositive cells along the microvessels in BrdU/CD31 double-stained sections. At least 3 microscopic fields were randomly sampled in each section.

To quantify the length and volume of brain microvessels, z-stack images were taken with the Olympus Fluoview FV1000 confocal microscope. A total of 10 consecutive images with the interspace of 1 μm and total volume of  $4.49 \times 10^5 \mu\text{m}^3$  were captured for each microscopic field. The imaging processing software Imaris was used to reconstruct three-dimensional images of BrdU and CD31 immunofluorescence. Briefly, images were imported into Imaris, and the CD31 immunosignal was remodeled to 3D images by the Filament operation. The Filament remodeling was processed with the four default steps in Imaris, including algorithm, preprocessing, segmentation, and graph compilation. All the images were processed with the same adjustments. The length, volume, and number of branches of CD31 immunofluorescence were calculated by Imaris based on the reconstructed 3D images.

### ***Neurobehavioral tests***

#### ***Adhesive removal test.***

The adhesive removal test was performed, as described previously<sup>17</sup> to assess forepaw sensitivity and motor impairments. Briefly, an adhesive tape (0.3 × 0.4 cm) was applied to the right forepaw to cover the glabrous region. The latency to touch the tape (time to touch) and completely remove the tape (time to remove) were recorded, with a maximum of 60 s. Mice were trained for

5 days before the dMCAO or sham surgeries. After surgery, this test was performed for up to 21 days. Three trials were performed on each testing day.

#### *Foot fault test.*

The foot fault test was performed, as described previously<sup>18</sup> to assess sensorimotor coordination during spontaneous locomotion. Mice were placed on an elevated grid surface (30 cm (L) × 35 cm (W) × 31 cm (H)), with a grid opening of 2.25 cm<sup>2</sup> (1.5 cm × 1.5 cm square) and videotaped for 2 min from below the grid. The videotapes were analyzed by a blinded investigator to count the number of total steps and the number of foot faults made by the right limbs (impaired side; contralateral to ischemic lesion). The number of total steps reflects gross locomotor function. Foot faults were determined when the mouse misplaced its right forepaw or hindpaw, such that the paw fell through the grid, and expressed as a percentage of total steps.

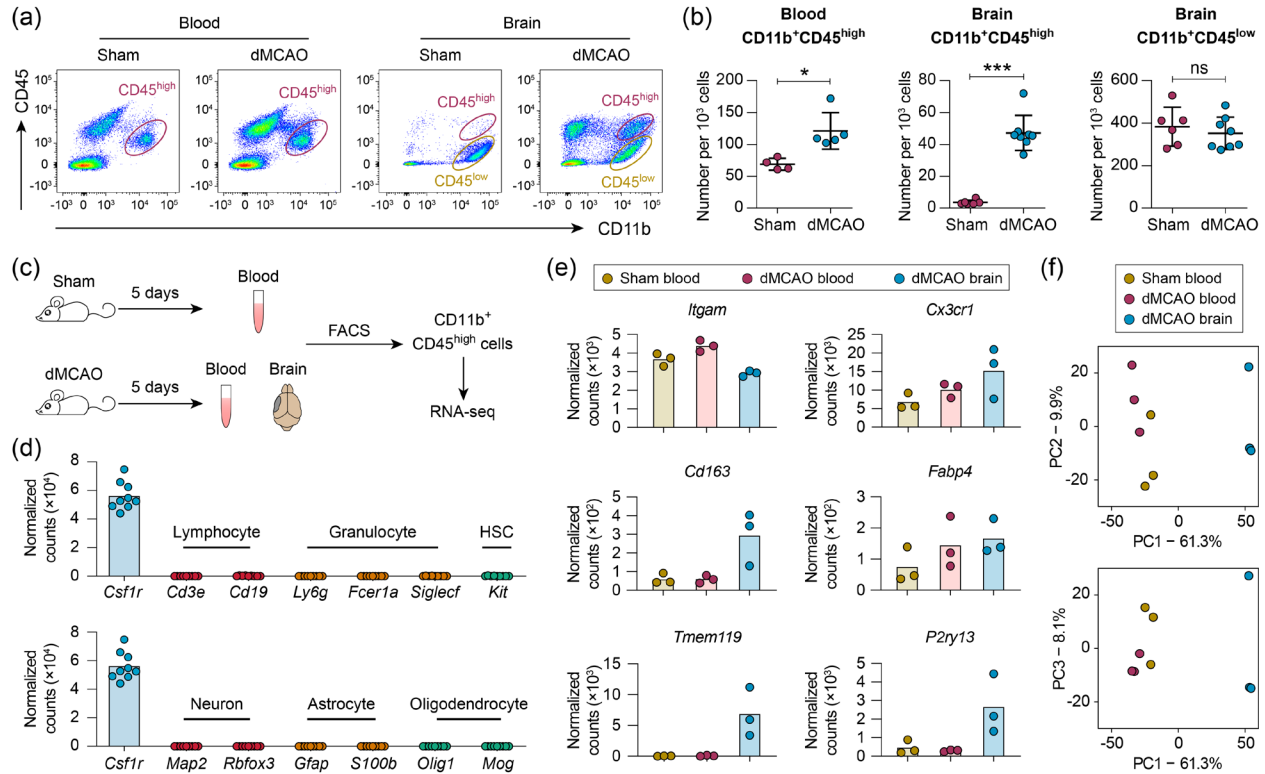
#### *Open field test.*

The open field test was performed to assess locomotor and anxiety-like behavior in mice before and up to 21 days after dMCAO. The mouse was placed into the Stoelting ANY-box open field area (40 cm × 40 cm) and allowed to freely explore the empty box for 5 min. Exploration was monitored via video tracking and the ANY-maze software (Stoelting Co.). The total distance traveled and time spent in the corner zones (defined as a 10 cm × 10 cm square zone in each of the 4 corners) were measured.

#### ***Data availability***

All RNA-seq data are deposited at GEO (NCBI). Other data that support the findings of this study are available from the corresponding author upon request. There are no restrictions on data availability.

## Supplementary Figures



### Supplementary Figure 1. RNA sequencing profiling of monocytes/macrophages in the mouse blood and brain after ischemic stroke.

(a,b) Mice were subjected to distal middle cerebral artery occlusion (dMCAO) or sham operation. The CD11b<sup>+</sup>CD45<sup>high</sup> (red oval) and CD11b<sup>+</sup>CD45<sup>low</sup> (yellow oval) cell populations in the blood and brain were quantified by flow cytometry 5 days after sham or dMCAO. Shown are representative density plots for CD11b and CD45 fluorescence after Ly6G<sup>-</sup>CD11c<sup>-</sup> gating (a) and summarized cell numbers (b). n=4-8 mice per group. \* $p < 0.05$ , \*\*\* $p < 0.001$ . ns, no significant difference. (c) Monocytes/macrophages (Ly6G<sup>-</sup>CD11c<sup>-</sup>CD11b<sup>+</sup>CD45<sup>high</sup> cells) were sorted from the blood and brain at 5 days after dMCAO or sham operation by FACS and subjected to RNA-seq. There were 3 biological replicates in each group. (d,e) RNA-seq expression profiles of established marker genes for various cell types in FACS-sorted cells. (d) FACS-sorted cells expressed low levels of markers for various blood cells (upper panel) and brain cells (lower panel) with comparison to the monocyte/macrophage marker *Csf1r*. HSC, hematopoietic stem cell. (e) Expression profiles of macrophage and microglia marker genes in FACS-isolated cells. Shown are the macrophage/microglia-common markers (upper panel; *Itgam*, *Cx3cr1*), macrophage-specific markers (middle panel; *Cd163*, *Fabp4*), and microglia-specific markers (lower panel; *Tmem119*, *P2ry13*). (f) Principal component analysis on RNA-seq expression profiles of FACS-sorted cells shows that samples in the same experimental group cluster together on principal component 1 (PC1).

## Supplementary Tables

### Supplementary Table 1. Key resources

REAGENT or RESOURCE	SOURCE	IDENTIFIER
<b>Antibodies</b>		
CD45 Monoclonal Antibody (30-F11), PerCP-Cyanine5.5	eBioscience	45-0451-82
CD11b Antibody, APC (Monoclonal, M1/70)	eBioscience	17-0112-83
Ly-6G Monoclonal Antibody (1A8), FITC	eBioscience	11-9668-82
BV421 Hamster Anti-Mouse CD11c, Clone HL3	BD Biosciences	562782
Purified Mouse Anti- BrdU	BD Biosciences	555627
Anti-NeuN (rabbit) Antibody	Millipore	ABN78
Purified Rat Anti-Mouse CD31	BD Biosciences	550274
Anti-MAP2 (clone AP20)	Millipore	MAB3418
Mouse CCL5/RANTES Antibody	R&D Systems	MAB478
Anti-mouse F4/80 Antibody, Clone BM8	Biolegend	123102
Rabbit anti-Iba1	Wako	019-19741
<b>Chemicals, Peptides, and Recombinant Proteins</b>		
Tamoxifen	Sigma-Aldrich	T5648
5-Bromo-2'-deoxyuridine (BrdU)	Sigma-Aldrich	B5002
<b>Critical Commercial Assays</b>		
RNeasy Plus Micro Kit	Qiagen	74034
SMART-Seq HT Kit	Takara Bio	634456
Nextera XT DNA Library Prep Kit Reference Guide	Illumina	15031942
Mouse on Mouse (M.O.M.) Basic Kit	Vector	BMK-2202
Neural Tissue Dissociation Kit (T)	Miltenyi Biotec	130-093-231
<b>Experimental Models: Organisms/Strains</b>		
Mouse: C57BL/6J	The Jackson Laboratory	Stock No: 000664
Mouse: B6.129P2(Cg)- <i>Cx3cr1<sup>tm2.1(cre/ERT2)Lit/J</sup></i> WganJ	The Jackson Laboratory	Stock No: 021160
Mouse: B6.129- <i>Pparg<sup>tm2Rev/J</sup></i>	The Jackson Laboratory	Stock No: 004584

<b>Oligonucleotides</b>		
Genotyping primer: Cx3cr1 <sup>CreER</sup> common GAA CTA CAA TCC TTT AAG GCT CAC G	This paper	N/A
Genotyping primer: Cx3cr1 <sup>CreER</sup> wild type GCA GGA CCT CGG GGT AGT CAC	This paper	N/A
Genotyping primer: Cx3cr1 <sup>CreER</sup> mutant CAC CAG AGA CGG AAA TCC ATC G	This paper	N/A
Genotyping primer: PPAR $\gamma$ <sup>loxP</sup> mutant reverse TGT AAT GGA AGG GCA AAA GG	The Jackson Laboratory	N/A
Genotyping primer: PPAR $\gamma$ <sup>loxP</sup> mutant forward TGG CTT CCA GTG CAT AAG TT	The Jackson Laboratory	N/A
<b>Software and Algorithms</b>		
Chipster v3.15	ref. <sup>5</sup>	<a href="https://chipster.csc.fi/">https://chipster.csc.fi/</a>
FastQC	ref. <sup>6</sup>	<a href="http://www.bioinformatics.babraham.ac.uk/projects/fastqc/">http://www.bioinformatics.babraham.ac.uk/projects/fastqc/</a>
HISAT2	ref. <sup>7</sup>	<a href="https://github.com/DaehwanKimLab/hisat2">https://github.com/DaehwanKimLab/hisat2</a>
HTSeq	ref. <sup>8</sup>	<a href="http://htseq.readthedocs.io/">http://htseq.readthedocs.io/</a>
R v3.5	ref. <sup>10</sup>	<a href="https://www.r-project.org/">https://www.r-project.org/</a>
DESeq2	ref. <sup>11</sup>	<a href="http://bioconductor.org/packages/DESeq2/">http://bioconductor.org/packages/DESeq2/</a>
Metascape	ref. <sup>12</sup>	<a href="http://metascape.org">http://metascape.org</a>
GOplot	ref. <sup>14</sup>	<a href="http://wencke.github.io/">http://wencke.github.io/</a>
clusterProfiler	ref. <sup>13</sup>	<a href="https://yulab-smu.github.io/clusterProfiler-book/index.html">https://yulab-smu.github.io/clusterProfiler-book/index.html</a>
Ingenuity Pathway Analysis	QIAGEN	N/A
FlowJo	FlowJo, LLC	N/A
ImageJ	NIH	N/A
Imaris	Bitplane	N/A
Prism 7.03	GraphPad	N/A

**Supplementary Table 2. Statistics reporting**

FIGURE	n	DATA STRUCTURE	TEST USED	STATISTIC	P VALUE
6(b) (CBF in perfusion unit)	6 mice (WT) 5 mice (mKO)	Normal distribution	Two-way ANOVA; Bonferroni <i>post hoc</i>	$F_{(1, 18)} = 0.6112$	ANOVA $p=0.4445$ mKO-WT>0.9999 (Baseline) mKO-WT>0.9999 (dMCAO)
6(b) (area)	6 mice (WT) 5 mice (mKO)	Normal distribution	Two-way ANOVA; Bonferroni <i>post hoc</i>	$F_{(1, 18)} = 4.671$	ANOVA $p=0.0444$ mKO-WT>0.9999 (Core) mKO-WT=0.2862 (Penumbra)
6(d) (BrdU <sup>+</sup> NeuN <sup>+</sup> cells)	4 mice WT sham) 4 mice (mKO sham) 8 mice (WT dMCAO) 9 mice (mKO dMCAO)	Normal distribution	One-way ANOVA; Bonferroni <i>post hoc</i>	$F_{(3, 21)} = 19.38$	ANOVA $p<0.0001$ mKO sham-WT sham>0.9999 mKO dMCAO-WT dMCAO=0.0006 WT dMCAO-WT sham<0.0001 mKO dMCAO-mKO sham=0.1402
6(d) (NeuN <sup>+</sup> cells)	4 mice WT sham) 4 mice (mKO sham) 8 mice (WT dMCAO) 9 mice (mKO dMCAO)	Normal distribution	One-way ANOVA; Bonferroni <i>post hoc</i>	$F_{(3, 21)} = 8.357$	ANOVA $p=0.0008$ mKO sham-WT sham>0.9999 mKO dMCAO-WT dMCAO>0.9999 WT dMCAO-WT sham=0.0154 mKO dMCAO-mKO sham=0.0088
6(f) (BrdU <sup>+</sup> CD31 <sup>+</sup> cells)	4 mice WT sham) 4 mice (mKO sham) 8 mice (WT dMCAO) 9 mice (mKO dMCAO)	Normal distribution	One-way ANOVA; Bonferroni <i>post hoc</i>	$F_{(3, 21)} = 30.03$	ANOVA $p<0.0001$ mKO sham-WT sham>0.9999 mKO dMCAO-WT dMCAO<0.0001 WT dMCAO-WT sham<0.0001 mKO dMCAO-mKO sham=0.1384
6(f) (branch number)	4 mice WT sham) 4 mice (mKO sham) 8 mice (WT dMCAO) 9 mice (mKO dMCAO)	Normal distribution	One-way ANOVA; Bonferroni <i>post hoc</i>	$F_{(3, 21)} = 1.295$	ANOVA $p=0.3022$ mKO sham-WT sham>0.9999 mKO dMCAO-WT dMCAO>0.9999 WT dMCAO-WT sham=0.4510 mKO dMCAO-mKO sham>0.9999
6(f) (vessel length)	4 mice WT sham) 4 mice (mKO sham) 8 mice (WT dMCAO) 9 mice (mKO dMCAO)	Normal distribution	One-way ANOVA; Bonferroni <i>post hoc</i>	$F_{(3, 21)} = 0.7836$	ANOVA $p=0.5164$ mKO sham-WT sham>0.9999 mKO dMCAO-WT dMCAO>0.9999 WT dMCAO-WT sham>0.9999 mKO dMCAO-mKO sham>0.9999
6(f) (vessel volume)	4 mice WT sham) 4 mice (mKO sham) 8 mice (WT dMCAO) 9 mice (mKO dMCAO)	Normal distribution	One-way ANOVA; Bonferroni <i>post hoc</i>	$F_{(3, 21)} = 0.3944$	ANOVA $p=0.7583$ mKO sham-WT sham>0.9999 mKO dMCAO-WT dMCAO>0.9999 WT dMCAO-WT sham>0.9999 mKO dMCAO-mKO sham>0.9999
7(a) (time to touch)	6 mice WT sham) 6 mice (mKO sham) 8 mice (WT dMCAO) 9 mice (mKO dMCAO)	Normal distribution	Two-way RM ANOVA; Bonferroni <i>post hoc</i>	$F_{(3, 25)} = 134.1$	mKO sham-WT sham>0.9999 mKO dMCAO-WT dMCAO<0.0001 WT dMCAO-WT sham<0.0001 mKO dMCAO-mKO sham<0.0001 dMCAO mKO-WT>0.9999 (Pre) dMCAO mKO-WT<0.0001 (3d) dMCAO mKO-WT<0.0001 (5d) dMCAO mKO-WT<0.0001 (7d) dMCAO mKO-WT=0.0042 (10d) dMCAO mKO-WT=0.0354 (14d) dMCAO mKO-WT=0.0126 (21d)
7(a) (time to remove)	6 mice WT sham) 6 mice (mKO sham) 8 mice (WT dMCAO) 9 mice (mKO dMCAO)	Normal distribution	Two-way RM ANOVA; Bonferroni <i>post hoc</i>	$F_{(3, 25)} = 170.9$	mKO sham-WT sham >0.9999 mKO dMCAO-WT dMCAO<0.0001 WT dMCAO-WT sham<0.0001 mKO dMCAO-mKO sham<0.0001 dMCAO mKO-WT>0.9999 (Pre) dMCAO mKO-WT<0.0001 (3d) dMCAO mKO-WT<0.0001 (5d) dMCAO mKO-WT<0.0001 (7d) dMCAO mKO-WT=0.0003 (10d) dMCAO mKO-WT=0.0145 (14d) dMCAO mKO-WT=0.0157 (21d)
7(b) (foot fault)	6 mice WT sham) 6 mice (mKO sham) 8 mice (WT dMCAO)	Normal distribution	Two-way RM ANOVA; Bonferroni <i>post hoc</i>	$F_{(3, 25)} = 297.7$	mKO sham-WT sham >0.9999 mKO dMCAO-WT dMCAO<0.0001 WT dMCAO-WT sham<0.0001

	9 mice (mKO dMCAO)		<i>hoc</i>			mKO dMCAO-mKO sham<0.0001 dMCAO mKO-WT>0.9999 (Pre) dMCAO mKO-WT=0.0001 (3d) dMCAO mKO-WT=0.0005 (5d) dMCAO mKO-WT=0.5810 (7d) dMCAO mKO-WT=0.0162 (10d) dMCAO mKO-WT=0.1162 (14d) dMCAO mKO-WT>0.9999 (21d)
7(b) (total steps)	6 mice WT sham) 6 mice (mKO sham) 8 mice (WT dMCAO) 9 mice (mKO dMCAO)	Normal distribution	Two-way RM ANOVA; Bonferroni <i>post hoc</i>	$F_{(3, 25)} = 1.579$		mKO sham-WT sham>0.9999 mKO dMCAO-WT dMCAO=0.4695 WT dMCAO-WT sham>0.9999 mKO dMCAO-mKO sham>0.9999
7(c) (total distance)	6 mice WT sham) 6 mice (mKO sham) 8 mice (WT dMCAO) 9 mice (mKO dMCAO)	Normal distribution	Two-way RM ANOVA; Bonferroni <i>post hoc</i>	$F_{(3, 25)} = 3.043$		mKO sham-WT sham>0.9999 mKO dMCAO-WT dMCAO=0.5124 WT dMCAO-WT sham>0.9999 mKO dMCAO-mKO sham=0.8650
7(c) (time in corner)	6 mice WT sham) 6 mice (mKO sham) 8 mice (WT dMCAO) 9 mice (mKO dMCAO)	Normal distribution	Two-way RM ANOVA; Bonferroni <i>post hoc</i>	$F_{(3, 25)} = 0.1625$		mKO sham-WT sham>0.9999 mKO dMCAO-WT dMCAO>0.9999 WT dMCAO-WT sham>0.9999 mKO dMCAO-mKO sham>0.9999
7(d)	8 mice (WT dMCAO) 9 mice (mKO dMCAO)	Normal distribution	<i>t</i> test (two-tailed)	$t_{(15)} = 0.7439$		mKO dMCAO-WT dMCAO=0.8684
7(e) (time to remove)	8 mice (WT dMCAO) 9 mice (mKO dMCAO)	Normal distribution	Pearson product-moment correlation	$r = -0.6604$		p=0.0039
7(e) (foot fault)	8 mice (WT dMCAO) 9 mice (mKO dMCAO)	Normal distribution	Pearson product-moment correlation	$r = -0.4217$		p=0.0918
7(f) (time to remove)	8 mice (WT dMCAO) 9 mice (mKO dMCAO)	Normal distribution	Pearson product-moment correlation	$r = -0.5820$		p=0.0142
7(f) (foot fault)	8 mice (WT dMCAO) 9 mice (mKO dMCAO)	Normal distribution	Pearson product-moment correlation	$r = -0.2177$		p=0.4012
7(g) (time to remove)	8 mice (WT dMCAO) 9 mice (mKO dMCAO)	Normal distribution	Pearson product-moment correlation	$r = -0.1679$		p=0.5194
7(g) (foot fault)	8 mice (WT dMCAO) 9 mice (mKO dMCAO)	Normal distribution	Pearson product-moment correlation	$r = -0.0074$		p=0.9776
S 1(b) (blood CD11b <sup>+</sup> CD45 <sup>high</sup> )	4 mice (Sham) 5 mice (dMCAO)	Non-normal distribution	Mann-Whitney <i>U</i> test (two-tailed)	$U = 0$		dMCAO-Sham=0.0159
S 1(b) (brain CD11b <sup>+</sup> CD45 <sup>high</sup> )	6 mice (Sham) 8 mice (dMCAO)	Non-normal distribution	Mann-Whitney <i>U</i> test (two-tailed)	$U = 0$		dMCAO-Sham=0.0007
S 1(b) (brain CD11b <sup>+</sup> CD45 <sup>low</sup> )	6 mice (Sham) 8 mice (dMCAO)	Normal distribution	<i>t</i> test (two-tailed)	$t_{(12)} = 0.6986$		dMCAO-Sham=0.4981

**Supplementary Table 3. Functional enrichment results of DEGs in monocytes from dMCAO blood versus sham blood.**

**Supplementary Table 4. Functional enrichment results of DEGs in monocytes/macrophages from dMCAO brain versus dMCAO blood.**

**Supplementary Table 5. GO enrichment results by *clusterProfiler* on vascular plasticity.**

Listed are GO terms (BP, CC, and MF) related to vascular plasticity that were significantly overrepresented by DEGs in monocytes/macrophages from dMCAO brain versus dMCAO blood.

**Supplementary Table 6. GO enrichment results by *clusterProfiler* on neuroplasticity.**

Listed are GO terms (BP, CC, and MF) related to neuroplasticity that were significantly overrepresented by DEGs in monocytes/macrophages from dMCAO brain versus dMCAO blood.

**Supplementary Table 7. Enriched GO terms related to vascular plasticity and neuroplasticity after reduction of overlap.**

**Supplementary Table 8. List of DEGs in macrophages from dMCAO brain versus dMCAO blood that were related to neurovascular plasticity.**

Listed are the 1034 genes that were differentially expressed, and genes under each of the 8 categories in Fig. 5A ranked according to adjusted p-values from lowest to highest.

## Supplementary References

1. Suenaga J, Hu X, Pu H, et al. White matter injury and microglia/macrophage polarization are strongly linked with age-related long-term deficits in neurological function after stroke. *Exp Neurol* 2015; 272: 109-119.
2. Pu H, Shi Y, Zhang L, et al. Protease-independent action of tissue plasminogen activator in brain plasticity and neurological recovery after ischemic stroke. *Proc Natl Acad Sci U S A* 2019; 116: 9115-9124.
3. Shi Y, Jiang X, Zhang L, et al. Endothelium-targeted overexpression of heat shock protein 27 ameliorates blood-brain barrier disruption after ischemic brain injury. *Proc Natl Acad Sci U S A* 2017; 114: E1243-E1252.
4. Li P, Gan Y, Sun BL, et al. Adoptive regulatory T-cell therapy protects against cerebral ischemia. *Ann Neurol* 2013; 74: 458-471.
5. Kallio MA, Tuimala JT, Hupponen T, et al. Chipster: user-friendly analysis software for microarray and other high-throughput data. *BMC Genomics* 2011; 12: 507.
6. Andrews S. FastQC: a quality control tool for high throughput sequence data. 2010. Available online at: <http://www.bioinformatics.babraham.ac.uk/projects/fastqc>.
7. Kim D, Langmead B and Salzberg SL. HISAT: a fast spliced aligner with low memory requirements. *Nat Methods* 2015; 12: 357-360.
8. Anders S, Pyl PT and Huber W. HTSeq--a Python framework to work with high-throughput sequencing data. *Bioinformatics* 2015; 31: 166-169.
9. Zerbino DR, Achuthan P, Akanni W, et al. Ensembl 2018. *Nucleic Acids Res* 2018; 46: D754-D761.
10. R Core Team. R: A language and environment for statistical computing. Vienna, Austria: R Foundation for Statistical Computing, 2018.

11. Love MI, Huber W and Anders S. Moderated estimation of fold change and dispersion for RNA-seq data with DESeq2. *Genome Biol* 2014; 15: 550.
12. Zhou Y, Zhou B, Pache L, et al. Metascape provides a biologist-oriented resource for the analysis of systems-level datasets. *Nat Commun* 2019; 10: 1523.
13. Yu G, Wang LG, Han Y, et al. clusterProfiler: an R package for comparing biological themes among gene clusters. *OMICS* 2012; 16: 284-287.
14. Walter W, Sanchez-Cabo F and Ricote M. GOplot: an R package for visually combining expression data with functional analysis. *Bioinformatics* 2015; 31: 2912-2914.
15. Kramer A, Green J, Pollard J, Jr., et al. Causal analysis approaches in Ingenuity Pathway Analysis. *Bioinformatics* 2014; 30: 523-530.
16. Pu H, Jiang X, Hu X, et al. Delayed Docosahexaenoic Acid Treatment Combined with Dietary Supplementation of Omega-3 Fatty Acids Promotes Long-Term Neurovascular Restoration After Ischemic Stroke. *Transl Stroke Res* 2016; 7: 521-534.
17. Zhao J, Mu H, Liu L, et al. Transient selective brain cooling confers neurovascular and functional protection from acute to chronic stages of ischemia/reperfusion brain injury. *J Cereb Blood Flow Metab* 2019; 39: 1215-1231.
18. Zhang J, Zhang W, Gao X, et al. Preconditioning with partial caloric restriction confers long-term protection against grey and white matter injury after transient focal ischemia. *J Cereb Blood Flow Metab* 2019; 39: 1394-1409.